General Disclaimer

One or more of the Following Statements may affect this Document

- This document has been reproduced from the best copy furnished by the organizational source. It is being released in the interest of making available as much information as possible.

- This document may contain data, which exceeds the sheet parameters. It was furnished in this condition by the organizational source and is the best copy available.

- This document may contain tone-on-tone or color graphs, charts and/or pictures, which have been reproduced in black and white.

- This document is paginated as submitted by the original source.

- Portions of this document are not fully legible due to the historical nature of some of the material. However, it is the best reproduction available from the original submission.

Produced by the NASA Center for Aerospace Information (CASI)

EFFECT OF BALL GEOMETRY ON ENDURANCE LIMIT IN BENDING OF DRILLED BALLS

BY

HAROLD E. MUNSON

TRW MARLIN ROCKWELL DIVISION

PREPARED FOR

NATIONAL AERONAUTICS AND SPACE ADMINSTRATION

NASA LEWIS RESEARCH CENTER

CONTRACT NAS3-17351

1. Report No. NASA CR-134930	2. Government Accession No.	3. Recipient's Catalog No.
4. Title and Subtitle EFFECT OF BALL GEOMETRY ON ENDURANCE LIMIT IN BENDING OF DRILLED BALLS		5. Report Date December 1975
		6. Performing Organization Code
7. Author(s) Harold E. Munson		8. Performing Organization Report No.
		10. Work Unit No.
9. Performing Organization Name and Address TRW Marlin Rockwell Division Jamestown, New York 14701		11. Contract or Grant No. NAS 3-17351
		13. Type of Report and Period Covered Contractor Report
12. Sponsoring Agency Name and Address National Aeronautics and Space Administration Washington, D. C. 20546		14. Sponsoring Agency Code

15. Supplementary Notes

Project Manager, Harold H. Coe, Fluid Systems Component Division
NASA Lewis Research Center, Cleveland, Ohio

16. Abstract

Four designs of drilled (cylindrically hollow) balls were tested in modified One Ball Test Machines for resistance to bending fatigue. Bending fatigue has been demonstrated to be a limiting factor in previous evaluations of the drilled ball concept.

A web-reinforced drilled ball was most successful in resisting bending fatigue.

Another design of through drilled design, involving a heavier wall than the standard reference ball, also showed significant improvement in resistance to bending fatigue.

Balls with carburized outer surfaces failed to demonstrate the improved resistance to bending fatigue to be expected of the lower hardness (brittleness) more material.

150-mm bore ball bearings, incorporating standard reference drilled balls and web-reinforced drilled balls, were operated at 20,000 RPM (3 million DN) at light to moderate axial loads. Erratic ball tracking and dynamic instability limited the performance of bearings with web-reinforced drilled balls at high speed and under heavy loads.

A 150-mm bore ball bearing, incorporating drilled balls with heavier than standard walls, was operated at 20,000 rpm (3 million DN) under 30480 newtons (6850 lbs) axial load for 28.9 hours. Testing was terminated by fracture of a drilled ball.

17. Key Words (Suggested by Author(s)) Ball bearings High speed Drilled ball Flexure fatigue		18. Distribution Statement Unclassified - unlimited
19. Security Classif. (of this report) Unclassified	20. Security Classif. (of this page) Unclassified	21. No. of Pages 22. Price* $3.00

* For sale by the National Technical Information Service, Springfield, Virginia 22161

NASA-C-168 (Rev. 10-75)

Table of Contents

ABSTRACT

Four designs of drilled (cylindrically hollow) balls were tested in modified One Ball Test Machines for resistance to bending fatigue. Bending fatigue has been demonstrated to be a limiting factor in previous evaluations of the drilled ball concept.

A web-reinforced drilled ball was most successful in resisting bending fatigue.

Another design of through drilled design, involving a heavier wall than the standard reference ball, also showed significant improvement in resistance to bending fatigue.

Balls with carburized outer surfaces failed to demonstrate the improved resistance to bending fatigue to be expected of the lower hardness (brittleness) bore material.

150-mm bore-ball bearings, incorporating standard reference drilled balls and web-reinforced drilled balls, were operated at 20,000 RPM (3 million DN) at light to moderate axial loads. Erratic ball tracking and dynamic instability limited the performance of bearings with web-reinforced drilled balls at high speed and under heavy loads.

A 150-mm-bore ball bearing, incorporating drilled balls with heavier than standard walls, was operated at 20,000 RPM (3 million DN) under 30480 newtons (6850 lbs) axial load for 28.9 hours. Testing was terminated by fracture of a drilled ball.

INTRODUCTION

Recent trends in gas turbine design and development have been toward engines with higher thrust-weight ratios and increased power output, which result in a requirement for high shaft speeds and larger shaft diameters. Bearings in current production aircraft turbine engines operate in the range from 1.5 million to 2.3 million DN (product of bearing bore in millimeters and shaft speed in rpm). Engine designers anticipate that turbine bearing DN values will increase to 3.0 million by 1980.

When ball bearings are operated at DN values above 1.5 million, centrifugal forces produced by the balls can become significant, by increasing Hertz stresses at the outer race-ball contacts, to seriously shorten bearing fatigue life. It is therefore logical to consider methods for reducing the factors that contribute to ball centrifugal loading, such as ball mass. Theory indicates that reductions in ball mass can be effective in extending bearing fatigue life at high speeds.

Both thin-wall spherically hollow and drilled balls have been evaluated in short time, high speed bearing experiments. The drilled ball concept, wherein ball mass is reduced as much as 50% by machining an accurate concentric hole through the ball, showed particular promise for 3 million DN bearing applications (refs 2,3,4).

Drilled balls, as compared with welded hollow balls, have several advantages:

(1) Fabrication is accomplished by standard ball processes;
(2) They can be easily inspected for flaws;
(3) Hole concentricity can be maintained very accurately, thus alleviating problems of ball unbalance at high speed; and
(4) A smooth surface finish can be achieved, without the irregularities present in the weld area of a spherically hollow ball.

In the designs of bearings incorporating drilled balls, special cages are required, with ball alinement restraints, to prevent the edge of the hole from damaging the race grooves during bearing start-up. (Reference 1)

Previous testing with drilled balls has been generally concerned with ball mass reduction of 50% (refs. 2,3,4,5). Such balls have experienced bending fatigue failures. Analyses of bending stress have demonstrated that, under maximum loads of normal main shaft bearing applications, drilled balls with 50% mass reduction do experience dangerously high stress (ref. 6). Analyses described in Ref. 4 indicate that 20.638-mm (.8125-inch) diameter balls, with 50% weight reduction are subjected to loads of approximately 900 lbs. in representative main shaft bearing applications.

This program was set up to evaluate drilled balls which should resist bending forces by virtue of heavier walls (less weight reduction), an internal reinforcing web, or more ductile metallurgical structure. Balls fabricated to incorporate these design features were run under relatively high radial loads in Modified One Ball Test Rigs. The most successful designs, from One Ball Test Rig results, was incorporated into 150-mm-bore ball bearings which were run at 3 million DN under thrust loads representative of the jet engine main shaft application.

BALL DESIGNS

Four designs of drilled balls were fabricated for this program. All were 20.638 mm-(.8125-in.) outer diameter. Designs A, B, C, Figures 1, 2 and 3 respectively, were made from a single batch of consumable-electrode, vacuum-melted AISI M-50 steel balls. Design D was identical in configuration to Design A but was made from one heat of AMS 9310 steel, carburized.

Design A balls were made to the same specifications as were the drilled balls reported by Holmes in Refs. 3 and 4. Data from testing these balls provided a reference against which the other designs could be compared.

Design B balls incorporated a stiffening web, perpendicular to the axis of the drilled hole and midway between the ends. The bore of the drilled hole was the same diameter as that in Design A, hence, Design B balls were somewhat heavier than Design A balls. Analyses performed at NASA's Lewis Research Center have indicated a substantial reduction in bending stress in the webbed configuration compared with the standard design (Ref. 6).

Design C balls had the same mass as Design B balls but had a straight-through bore. Therefore, these balls possessed a heavier cross-section than did the reference balls.

Design D balls had essentially the same mass and cross section as the reference balls, but were made from carburized AISI 9310 steel.

Measured masses of representative balls of the various designs were:

	MASS	PERCENT OF ORIGINAL MASS	PERCENT MASS REDUCTION
Solid Ball	35.8228 grams	100.0	-------
Design A	17.3342 grams	48.4	51.6
Design B	19.1848 grams	53.6	46.4
Design C	18.8274 grams	52.6	47.4
Solid Carburized Ball	35.9727 grams	100.0	-------
Design D	17.4150 grams	48.4	51.6

Drilled balls were fabricated from AFBMA Grade 10 balls. Two parallel flats 14.5-millimeters (.571-in.) apart and equidistant from a parallel plane through the center of the ball were ground on each ball. Then balls were drilled, perpendicular to the parallel flats, by a combination of electric discharge machining (EDM) and conventional grinding.

In the first 50 design A balls, the diameter of the EDM holes was 12.4-millimeters (0.488-in.). The holes were then finish ground to 12.57-millimeters (0.495-in.). The edges of the hole were chamfered and corners were blended. After a number of early failures were experienced in these balls, 16 more were processed by installing 11.43-millimeters (0.450-in.) diameter holes by EDM, then grinding to finish size. Concentricity of the finished hole was maintained to within 0.025-millimeter (0.001-in.). Surface finish of the hole was held to 0.15-micrometer rms (6-μ in. rms).

Design B balls were all drilled after the question of adequate grinding allowance had arisen. It was necessary to drill in from both ends, stopping at planes equidistant from the ends, to provide an interior wall or "web". The holes produced by EDM were 11.43-millimeters (0.450-in.) diameter and stopped short of the

finished web by .51 - .64-mm (0.020-0.025-in.). The holes were then finished by grinding to an 0.15-micrometer rms (6-μ in. rms) surface, and corners were blended.

Design C balls were drilled straight through by EDM, providing an 11.8-mm (0.465-in.) diameter hole. This hole was then finish ground to 12.0-mm (0.472-in.) diameter, and corners were blended. As in other designs, hole concentricity was held to within 0.025-mm (0.001-in.) and surface finish of the hole and ends was within 0.15-micrometer rms (6-μ in. rms).

Design D balls were drilled to the same specifications as were the second group of Design A balls, above.

TEST BEARINGS

The test bearing specifications are listed in Table I. The bearings were 150-mm-bore, angular-contact, split-inner-race ball bearings with 20.64-mm (0.8125-in.) diameter balls. The one-piece machined cages were located on the outer race and incorporated machined restraining ribs in the ball pockets to locate the drilled balls. (Ref. 5). These ribs restricted twisting movement of the ball to about 37° and prevented the edge of the hole from riding on the race groove during bearing operation.

In each mating face of the inner-race halves, there were 12 radial slots of 1.3-mm (0.050-in.) radius extending from the bore to the raceway.

APPARATUS AND INSTRUMENTATION
BALL TEST APPARATUS

Dynamic testing of individual balls was conducted on special One-Ball Test Rigs, shown schematically in Figure 4. A 1.5-kw (2-HP), 220/440 volt, three-phase electric motor with an integral variable-sheave speed changer, drove each test rig through a V-belt. Rig speed was infinitely variable from approximately 900 rpm to the scheduled 7,700 rpm. At a shaft speed of 7,700 rpm, ball rotational speed was approximately 39,500 rpm. Figure 5 is a photograph of a test machine.

A test ball was loaded between two bearing inner races, one of which was mounted on the main shaft of the rig, and the other was mounted on an idler shaft. Each race corresponded to the inner race of a light-series, deep-groove, 90-mm-bore ball bearing (MRC 218-S). Races were made from AISI 52100 steel and their radii of curvature were 52% of ball diameter. Load was accomplished by a hydraulic cylinder pushing through the rig's idler shaft. An accumulator in the load system minimized load variation due to thermal effects.

Each ball was positioned by a separator block. At the forward end of this ball "pocket" was mounted a small arbor with its axis parallel to the race axis. The test ball contacted a circumferential V-groove in this arbor. As the ball rotated, it was prevented from rolling out of position by the arbor, which was mounted on 10-mm bore, extremely light series, deep-groove, ball bearings (MRC 1900-S). This eliminated most of the sliding friction between ball and guide. The contact between ball and arbor occurred along two lines which were outside of the ball-race contact.

Maximum speed of this positioning arbor was approximately 60,000 rpm at full rig speed.

The lubrication system included an oil sump with electric heating elements, a supply pump and a filter. Oil, Mobil Jet II, meeting specification MIL-L-23699B was jetted into the test ball at 0.9 kg (2 lbs.) per minute. Temperature of the test oil was 389 K (240° F.). Additional quantities of the same oil were used to lubricate support bearings.

In later testing, a V-groove race with 100° included angle was substituted for the upper race. Several Design B balls were run in the rigs between one conventional race and one V-groove race. This was done to provide off-set loading tests.

BEARING TEST RIG

Dynamic testing of the 150-mm-bore ball bearings was conducted on the three-bearing test spindle shown schematically in Figure 6. Figure 7 is a photograph of the spindle, with oil lines and instrumentation attached. A 56-kw (75-HP), 440-volt, three-phase AC electric motor with integral variable pitch pulleys and belts drove the rig. Between the drive unit and the spindle were a magnetic coupling and 5X geared speed increaser. Minimum stabilized speed of the arrangement was 7,000 rpm; however, the magnetic coupling permitted this speed to be reached over a period of about one minute after start up. Thereafter, speed was infinitely variable through 20,000 rpm.

The test bearing was cantilever mounted on the test spindle, as shown on Figure 6. The bearing was mounted on the shaft with a 0.0635-mm (0.0025-in.) interference fit.

Thrust load was applied to the test bearing by pressurizing a hydraulic cylinder connected to the bearing housing by a 0.71-meter (28-in.) length of 7.9-mm (5/16-in.) diameter cable. This method of loading minimized possibilities of misalinement and produced only slight torque tare. The thrust load produced by the hydraulic cylinder was calculated from pressure gage readings. Reaction to the thrust load was provided by an 80-mm-bore ball support bearing. This ball bearing and another 80-mm-bore ball bearing provided radial support for the shaft. A preload spring, plus a sliding housing fit for the outboard support bearing maintained axial preload on the support bearings at all times, assuring radial rigidity.

The lubrication system included a common oil sump with electric heating elements, a supply pump, and a filter. Separate oil supply lines were used for the support bearings and the test bearing. The oil supply to the test bearing was heated or cooled as necessary to maintain a constant oil inlet temperature of 389K (240° F). Support bearing oil had an additional cooler to provide lower oil inlet temperature to the support bearings. All lubricant and coolant to the test bearing was jetted into an oil scoop in the bore of the hollow shaft. Oil reached the outer diameter of the shaft near the unloaded half of the inner race, then passed under the inner race through 12 equally spaced axial passages, each 2.38-mm (0.0938-in.) deep by 4.78 mm-(0.188-in.) wide. At the juncture of the two inner race halves, a portion of the oil was forced, by centrifugal force, into the bearing through radial passages at the interface.

The remaining oil passed on to the end of the axial passages and was discharged separately. During actual testing, most of the oil entered the bearing. Multiple oil-outlet holes were provided on each side of the bearing housing for lubricant scavenge, and additional multiple holes were provided for cooling-oil scavenge. Oil-inlet flow rate was measured by a volumetric-type flow meter. Oil-outlet flow rates were measured at intervals by graduated cylinder and stop-watch.

Temperatures were measured by Chromel-Alumel thermocouples and recorded on millivolt strip-chart recorders. Temperatures were measured at the following locations:

(1) Oil-inlet
(2) Test bearing outer ring
(3) Oil-outlet on the inboard side of the test housing
(4) Oil-outlet on the outboard side of the test housing
(5) Oil-outlet for test bearing under race cooling oil
(6) Oil sump
(7) Outer rings of both support bearings

Individual oil-outlet temperatures were measured in the lines from the test bearing which came out at the six o'clock positions and thermocouples were located 5.1 to 7.6-centimeters (2 to 3-in.) from the bearing. All bearing and oil temperatures were accurate to within $\pm$ 1K ($\pm$ 2° F.) of the indicated readings.

The torque of the test bearing was measured by using a strain-gage mounted on the restraining arm. The strain-gage signal was amplified and recorded. The force, determined from the strain-gage readings multiplied by the length of the torque arm, represented the bearing torque. The recorded torque was corrected for the rotation induced on the load cable by axial load.

Speed was measured by a magnetic pick-up, with the signal displayed on an electronic counter.

BALL TEST PROCEDURE

Each test ball was run between new pairs of races, (except in a few tests in which an infant failure problem was being investigated). The separator was changed only when it was damaged, which frequently occurred with ball breakage.

Before start-up, oil was preheated to approximately 339K (150° F.) and jetted into the test location at .9 kg (2 lbs.) per minute. Approximately one-third of the scheduled load was applied and the rig was started at minimum speed. The oil temperature was advanced to 389K (240° F.) as rapidly as possible. Speed was then increased to full value, 7,700 rpm. Load was increased to scheduled value over a period of several minutes.

Balls were run to failure or to run-out, the latter being 250,000,000 cycles which required 53 hours running for normal tests, or 500,000,000 cycles (106 hours running), for endurance tests. At failure, there was an increase in vibration, highly audible, which triggered an automatic shut down device.

Basic procedure with each lot of balls was to run five balls under 6,008 newtons (1,350 lbs.) radial load to failure or for 53 hours. If any failures occurred, five more balls were run at 5,340 newtons (1,200 lbs.). If any failures occurred at the second load condition, five more balls were run at 4,005 newtons (900 lbs.) radial load.

If a group of five balls all achieved scheduled run-out, at one load level, five more balls from the same lot were run under that same load until failure, or for 106 hours.

These procedures were varied slightly because of the incidence of premature, or infant, failures in two lots, (A and C) and because of very poor performance in Lot D. In testing Design A and Design C balls, premature failures were disregarded in determination of the ability of a ball to withstand a particular load. In testing Design D balls, fewer than five balls were tested at each of the scheduled heavier loads and more were tested at the lowest load (4005 newtons).

In supplemental testing, Design B balls were run one at a time, between one conventional race and one V-groove race, under the following radial loads, and resulting contact stresses (at the V-groove interface):

LOAD	MEAN HERTZ STRESS
6,008 newtons (1,350 lbs.)	303,000 N/cm^2 (440,000 psi)
5,340 newtons (1,200 lbs.)	293,000 N/cm^2 (425,000 psi)
4,450 newtons (1,000 lbs.)	276,000 N/cm^2 (400,000 psi)
3,560 newtons (800 lbs.)	255,000 N/cm^2 (370,000 psi)

Two balls were tested at each load.

BALL TESTING

Results of testing individual balls are summarized on Table II.

SHAKEDOWN TESTS

Three Design A drilled balls were run at varying speeds and loads up through the maximum scheduled. One ball in each machine ran for several hours under a variety of conditions, including numerous starts and stops, then ran for several hours under maximum conditions. The third shakedown ball failed after 1.2 hours. This ball was subjected to an overload condition during start-up.

TESTING OF DESIGN A BALLS

Five balls were run under 6,008 newtons (1,350 lbs.) radial load with three bending fatigue failures, and two suspensions at scheduled run-out. These data are plotted on Figure 6.

Five balls were then run under 5,340 newtons (1,200 lbs.) radial load to scheduled run-out.

However, several balls, intended for testing under either 6,008 or 5,340 newtons (1,350 or 1,200 lbs.) radial load, experienced bending fatigue failure shortly after start, before scheduled load had been applied. These were designated "infant failures" and investigations were conducted to determine the cause.

The first infant failures had occurred when oil was preheated to 389 K (240° F) before start of testing. Thereafter, testing was started with cooler oil and scheduled temperature was not reached until the ball had attained full speed and load. Subsequent infant failures under revised start-up procedures demonstrated that thermal shock was not the cause.

In a further attempt to eliminate thermal conditions as a possible cause of early failure, the lubricating system was modified to jet part of the oil to the bore of the ball. Infant failures continued to occur after this modification.

The possibility that characteristics of individual test machine races were contributing to early failures was investigated. Examination of races indicated no discrepancies. A few races were re-run with new balls, after an infant failure. No pattern was established. On the other hand, two race failures occurred during the course of testing long life balls; in both cases, the spalled race was replaced and the ball was left in test; scheduled run-out was achieved with both balls.

A possible cause of early ball failure was the effect of a residual heat-affected zone, resulting from the EDM operation. Design C balls and part of the Design A balls were drilled with EDM, leaving 0.15 - 0.20-mm (.006 - .008-in.) diametral stock for clean-up by conventional grinding and finishing. Experience in which the grinding stock allowance had not been sufficient for clean-up caused diametral allowance to be increased to 1.14-mm (.045-in.). Several Design C balls had failed to pass our visual inspection of the bores, but regrinding an additional 0.051-mm (.002-in.) diametral stock had removed all visible evidence of EDM.

Metallurgical examination of an infant failure revealed no residual heat-affected zone. Metallurgical examination of a ball which had been drilled, but not ground, showed a heat-affected zone of 0.04-mm (.0016-in.) depth.

Sixteen additional Design A balls were obtained which had 1.14-mm (.045-in.) diametral stock removal by grinding. Ten of these balls were tested, with no infant failures. Fatigue endurance data at 6,008 newtons (1,350 lbs.) radial load for these balls are also plotted on Figure 8. These data are not significantly different from those obtained on the original lot of balls of the same design, when infant failures are disregarded.

Failures occurring on the second lot of Design A balls under 5,340 newtons (1,200 lbs.) radial load indicated that this design was inadequate for that load. Since Design B and C balls had demonstrated capability of satisfactory operation at 6,008 newtons (1,350 lbs.), testing of Design A balls was terminated.

TESTING OF DESIGN B BALLS

Five Design B balls (incorporating a reinforcing web) were run to scheduled shut-down at 250,000,000 cycles under maximum load, 6,008 newtons (1,350 lbs.). Five more Design B balls were then run to shut-down at 500,000,000 cycles under the same load. There were no failures in Design B balls during this testing.

In a further evaluation, to determine the effect of a high angle contact load on the Design B ball, ten balls were run between a standard race and a V-groove. Loads were heavy enough to produce rolling contact fatigue failures, as well as bending fatigue failures, at the V-groove interface. Under the two higher loads, life was measured in minutes. At failure, a chunk of the ball tended to break out. In one of the balls tested at 5,340 newtons (1,200 lbs.), the failure appeared to have started as a contact fatigue spall, and the test was stopped before cracked areas at the bore had actually broken loose. Lives at 4,450 and 3,560 newtons (1,000 lbs. and 800 lbs.) radial load were longer, significantly so at the lowest load. Failures started as spalls, with cracks then progressing to the bore. (See Figure 9). One test was stopped before cracks from the spall had reached the bore. (See Figure 10).

In V-groove testing, the center of the contact ellipse was .093 radians (5° 21') from edge of ball. Under 6008 newtons (1350 lbs.) load, edge of contact ellipse was approximately 0.28-mm (.011-in.), circumferentially from the edge of ball.

TESTING OF DESIGN C BALLS

Design C balls were drilled with 0.15 - 0.20-mm (.006 - .008-in.) stock removal by grinding after the EDM operation. Several of the balls showed tiny pits in the bore when first received; they were subsequently reground to the maximum diameter of our tolerance, 0.051-mm (.002-in.) diametral increase, which removed all indication of the pits.

Six of the reground balls, above, were put into test under 6,008 newtons (1,350 lbs.) load. Four of them achieved 250,000,000 cycles and two suffered infant failures.

Two other Design C balls also experienced infant failures.

Except for the infant failures, all Design C balls reached scheduled shut-down, at 250,000,000 or 500,000,000 cycles, under 6,008 newtons (1,350 lbs.) load.
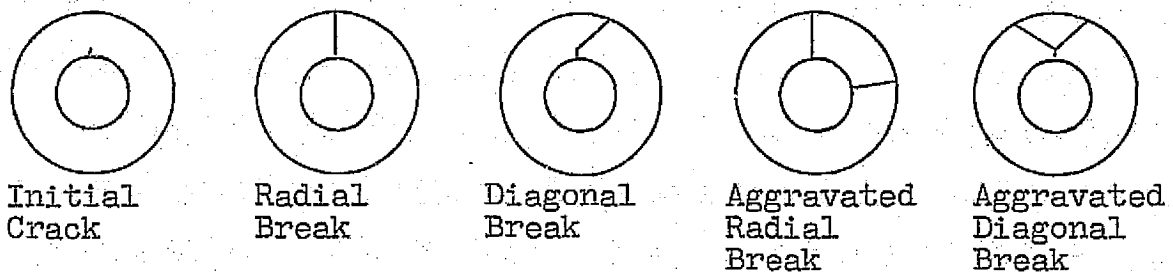
TESTING OF DESIGN D BALLS

Design D balls were identical in configuration to Design A balls, but differed in material. It was expected that crack arresting properties of the AISI 9310 steel would result in a drilled ball which was more resistant to bending fatigue.

Two each were tested at 6,008 and 5,340 newtons (1,350 and 1,200 lbs.) load with very short lives. Nine balls were tested at 4,005 newtons (900 lbs.) load with lives ranging from the infant failure area to run-out at 250,000,000 cycles.

Testing of Design D balls was suspended because of poor performance.

INSPECTION OF BALL FAILURES

Examination of ball failures indicated that fractures started at the bore, then progressed more or less radially outward. Figure 11 shows a ball failure in which the crack is only in the bore. In some breaks the crack was distinctly radial. In others the crack moved outward at an angle from a true radial plane. The two break patterns are described as "radial" and "diagonal" in Table II. A pictorial representation of the various break patterns is shown below:

Initial   Radial   Diagonal   Aggravated   Aggravated
Crack   Break   Break   Radial   Diagonal
                                      Break   Break

If a ball with diagonal break was permitted to run for a few seconds, a second diagonal break would often occur. The resulting chunk would drop out of the ball. See Figures 12 and 13 for representative failures.

If a ball with a radial break were permitted to run for a few seconds, another radial break would often occur, with a catastrophic failure. (See Figure 14).

Within a few seconds of running after a break had occurred, friction at the interface of the break would result in high localized temperatures. (See Figure 15).

In Design D balls, breaks tended to be non-planar, as contrasted with breaks in the through-hardened balls. Figures 16, 17, and 18 show characteristic failures in Design D balls.

Design B balls were most successful in that no failures occurred under originally scheduled testing. When these balls were run under very high Hertz stresses against a V-groove race, the reinforced design demonstrated an ability to retain structural integrity after failure had initiated. Figures 9 and 10 show spalls on Design B balls run against a V-groove race.

Except for infant failures, which were attributable to insufficient clean-up of EDM effects, Design C balls were also successful in meeting load-life requirements.

BEARING TESTING

Two sets of bearings were tested; the first set had Design B balls, while the second set used Design C balls.

Bearing test conditions were:

```
Speed        - 20,000 RPM
Load         - 20,480 newtons (6,850 lbs.) axial
Lubrication  - MIL-L-23699B oil (Mobil Jet II) at
               0.00757 meter³ per minute (2 gallons
               per minute)
Temperature  - Oil-in at 389 K (240°F)
Duration     - Failure or 100 hours
```

BEARINGS WITH DESIGN B BALLS

Bearings incorporating Design B balls were run at 20,000 rpm (3,000,000 DN) but were unable to operate at scheduled load, 30480 newtons (6,850 lbs.). Several tests were made. In each test, one or more balls tilted excessively, wearing into the restraining ribs in the ball pocket, and abrading one or both sides of the ball. (See Figures 19 and 20.) With the braking action which occurred at this time, there was light skidding on the races. In each case, audible indications of bearing distress were observed as load was being increased through the 15,575 newtons (3,500 lbs.) range.

Several short runs, using modified procedures or test specimens, were made to clarify the problem. Decreasing contact angle to approximately 20° (by intermatching inner and outer rings between bearings) resulted in the same sort of damage at the same operating conditions as had occurred when contact angle was approximately 31°.

In another run, the 20° contact angle, rematched bearing, was complemented with Design A balls. It was recognized that some of the balls might be prone to infant failure. At 24,475 newtons (5,500 lbs.) thrust load, audible indications of bearing distress were heard. The

bearing was permitted to run for a few minutes longer at loads between 15,575 and 20,025 newtons (3,500 and 4,500 lbs.) but testing was terminated when further noise was heard. Upon disassembly, a broken ball was found but none of the balls had tilted enough to contact a pocket restraining rib.

The following torque values were obtained during testing of the rematched 9130UK29 bearing using Design A balls, at 20,000 RPM.

LOAD	TORQUE
16,020 newtons (3,600 lb.)	10.71 N-m (7.9 ft. lb.)
18,330 newtons (4,120 lb.)	10.99 N-m (8.1 ft. lb.)
20,470 newtons (4,600 lb.)	11.66 N-m (8.6 ft. lb.)
22,920 newtons (5,150 lb.)	11.93 N-m (8.8 ft. lb.)
24,475 newtons (5,500 lb.)	11.66 N-m (8.6 ft. lb.)

During the course of bearing testing, both bearings were damaged. Multiple runs on the same bearing were achieved by rehoning races, replacing damaged balls, and reversing orientation of cages.

Design B balls, which tilted excessively in test, generally shifted so that the plane of the reinforcing web turned in the direction of the contact angle. Then they continued to tip until they scrubbed the restraining ribs of the pockets. However, a ball in one test tilted in the opposite direction.

Apparently the Design B balls become dynamically unstable under angular contact and high load. Perhaps the deflection of the ball at the inner race contact, with much lesser deflection at the outer race contact (due to the load position with respect to the reinforcing web) creates a couple which is sufficient to overcome the effects of inertial forces.

BEARING WITH DESIGN C BALLS

An MRC 9130-UK29 ball bearing was assembled with Design C drilled balls in further efforts to achieve 3 million DN operation under high axial load.

Races from the rematched, 20° contact angle bearing (used with Design B balls) were honed to remove evidence of previous running. The contact angle of the bearing after rehoning was 21°. A new cage was procured.

New Design C balls, which were drilled with 1.14-mm (.045-in.) grinding stock allowance, were obtained to complement the bearing.

The bearing operated for a total of 28.9 hours at full speed and load, 20,000 rpm and 30480 newtons (6,850 lbs.). In addition it operated for 16.8 hours at lower speeds and/or loads during start-ups and rig check outs. There were a total of twenty-one starts and shut-downs

during the course of this operation.

Testing was terminated when one drilled ball fractured.

During the course of testing, average values of significant parameters, measured at full load and speed were:

Oil-in Temperature   - 389K $(240^\circ F)$
Oil-out Temperature - 439K $(331^\circ F)$

Bearing Outer Race Temperature - 527K $(490^\circ F)$
Bearing Torque   - 12.2 to 12.7 N-m
                                                     (9.0-9.4 ft/lbs)

Failure was indicated by noise. The test rig was permitted to operate for perhaps 30 seconds after the first change in noise, during which time the outer race temperature increased 17K $(30^\circ F)$.

Examination of the bearing revealed that one ball had broken into several pieces. See Figure 21. In addition, all balls had tilted in their pockets with the result that the sides of the balls scrubbed heavily into the alinement restraints in both sides of each pocket. All balls had tilted in the same basic orientation - so that the axis of a drilled ball was essentially perpendicular to the line of contact from outer race through the ball to inner race. Markings on the sides of the broken ball indicated that it had also scrubbed on the cage alinement restraints before it collapsed.

Apparently, the initial cracking of the failed ball threw the bearing into an unstable operational mode; the bearing continued to run until manual shut down, by which time the one ball had received multiple fractures.

The bearing had been completely disassembled and examined after approximately 20 hours and again after 25 hours of full speed-full load operation. These examinations showed a number of dents in balls and races and some incidental contact between sides of drilled balls and pocket restraints, but no serious damage. Figure 22 is a photograph of a section of the cage taken at the 20 hour examination, showing only normal wear.

Figure 23 shows a Design C ball as removed from the failed bearing at 28.9 hours. Figure 24 shows a section of cage with severely damaged alinement restraints, after test; balls in the section of cage shown were unbroken but severely scrubbed.

Land riding surfaces of the cage showed contact with the outer ring. In one area this contact had worn through the silver.

Races showed incidental dents and minor skidding damage. Based on examinations of the bearing during the course of the run, the skid damage probably occurred at failure. The lands of the outer race were well polished from contact with the O.D. of the cage.

The dynamic instability which occurred in the test bearing, with Design C balls, after initiation of failure, produced the same sort of damage to balls and cage as occurred in bearings with Design B balls. One may speculate that the initial crack in fractured Design C ball started at the bore and proceeded to the sides in the same manner as occurred during single ball tests; during the short interval when the heaviest section of the ball was intact but the sides were fractured, its deflection characteristics were changed and a couple was created by the race contact forces.

While a change in deflection characteristics can explain the damage which occurred to the sides of the fractured ball, before it collapsed, it does not explain the dynamic instability of the remaining balls. P. W. Holmes, in Ref. 3, noted that drilled balls dimensionally the same as Design A balls, tilted excessively at high loads, and low speeds. Experience with Design B balls under angular contact in this program indicated a relationship between tilting and load. It appears that excessive deflection or collapse of a single ball could result in additional load on adjacent balls. When a drilled ball tilts sufficiently to contact a cage restraint its deflection under load changes so that other balls are more heavily loaded. The chain reaction which develops could cause all balls to tilt.

An alternative possibility - that balls tilted before the initial bending fatigue fracture occurred - appears unreasonable.

At no time during the final few hours of operation did a high load - low speed condition occur. An emergency shut down under full load was effected at 25 hours, but subsequent examination revealed nothing but incidental contact between balls and restraints. Temperature data also indicate no abnormal trends until the final minute of operation.

The heavy walled drilled ball, Design C, demonstrated a capability of operating for a significant period of time in a ball bearing at 3 million DN under loads comparable to the maximum occurring in main shaft jet engines. In this respect, it is superior to Design A (standard drilled ball) and Design B (web reinforced design). Scheduled life of 100 hours was not achieved in this program, and a design with greater resistance to bending fatigue is required.

CONCLUSIONS

The drilled ball concept has demonstrated the capability of operating satisfactorily in bearings which rotate at three million DN. However, initial designs, with about 52% mass reduction, are not strong enough to

resist bending fatigue present in jet engine main shaft applications.

The webbed ball design demonstrated excellent resistance to bending fatigue. Testing under high rolling contact stresses, concentrated near an edge of the drilled ball, indicated that rolling contact fatigue does not immediately result in catastrophic failure. However, the webbed ball appears to be dynamically unstable when operating under high loads in an angular contact ball bearing.

The heavier walled ball, Design C of this program, with 47.4% mass reduction, demonstrated significantly improved bending fatigue resistance over the initial design.

A bearing incorporating these balls operated at three million DN under heavy axial load for 28.9 hours. Failure of this bearing was due to fracture of a ball. It appears that a still heavier walled design, or a more fatigue resistant material is required for general application of the concept.

Results of this program also demonstrate the need for special precautions in the use of electric discharge machining (EDM) in highly stressed bearing components. Accepted industry practices for grinding stock allowance, subsequent to the EDM operation, are apparently inadequate. Further investigation in this area is needed.

26

REFERENCES

(1) Irwin, Arthur S.: "Drilled Ball Bearing with a One
Piece Anti-Tipping Cage Assembly".
U.S. Patent No. 3,905,660, 1975.

(2) Coe, Harold H.; Scibbe, Herbert W.; and Anderson,
William J.: Evaluation of Cylindrically Hollow
(Drilled) Balls in Ball Bearings
at DN Values to 2.1 Million. NASA
TN D-7007, 1971

(3) Holmes, P. W.: Evaluation of Drilled Ball Bearings
At DN Values to Three Million.
I - Variable Oil Flow Tests. NASA
CR-2004, 1972

(4) Holmes, P. W.: Evaluation of Drilled Ball Bearings
at DN Values to Three Million.
II - Experimental Skid Study and
Endurance Tests. NASA CR-2005, 1972

(5) Scibbe, Herbert W.; Munson, H. E.:
Comparison of Experimental and
Predicted Performance of 150-
Millimeter-Bore Solid and Drilled
Ball Bearings to 3 Million DN. NASA
TN D-7737, 1974.

(6) Coe, Harold H.; and Lynch, John E.:
Analysis of Stresses at the Bore
of a Drilled Ball Operating in a
High-Speed Bearing. NASA TN D-7501,
1973

TABLE I

SPECIFICATIONS FOR MRC 9130 - UK - 29 BALL BEARINGS

Bearings were made to Annular Bearing Engineers Committee
grade 5 tolerances.

RINGS AND BALLS	
Material	Consumable-electrode, vacuum-melted AISI M-50 steel
Hardness	Rockwell C 60 to 63
Inner-race bore, mm (in.)	150 (5.9053)
Outer-race outside diameter, mm (in.)	225 (8.8583)
Width, mm (in.)	35 (1.3780
Number of balls	24
Ball outside diameter, mm (in.)	20.638 (0.8125)
Pitch diameter, nominal, mm (in)	186.89 (7.3578)
Contact angle, nominal, rad (deg)	0.5110 (29.28)
Radial clearance under 147-N (33-lbf) load, mm (in.)	0.107 to 0.142 (0.0042 to 0.0056)
Inner-race radius, percent of ball diameter	52
Outer-race radius, percent of ball diameter	51
CAGE	
Material	SAE 4340 steel, silver plated 0.025 to 0.051-mm (0.001 to 0.002-in) thick per AMS-2412
Hardness	Rockwell C28 to 32
Cage width, maximum, mm (in)	28.04 (1.104)
Ball-pocket clearance, diametral, mm(in)	0.635 to 0.838 (0.025 to 0.033)
Cage-land clearance, diametral, mm(in)	1.02 (0.040)

TABLE II
SUMMARY OF DRILLED BALL TESTING

| DESIGN	BALL NO.	MACHINE	LOAD	HOURS	STATUS
A	1	1	Varied	41.5	Shakedown ball, no failure
A	2	2	Varied	22.0	Shakedown ball, no failure
A	3	2	Varied	1.2	Shakedown ball, radial break
A	4	2	------	0.2	Diag. break; infant failure
A	5	1	------	0.2	Diag. break; infant failure
A	6	2	6008N	46.3	Radial break; 2.5 hrs. at reduced loads
A	7	1	6008N	38.3	Radial break
A	8	1	6008N	14.1	Radial break
A	9	2	6008N	53.5	No failure, suspended
A	10	1	6008N	53.5	No failure, suspended
A	11	1	------	0.1	Diag. break; infant failure
A	12	2	5340N	53.5	No failure, suspended
A	13	1	------	0.1	Rad. break, infant failure
A	14	1	5340N	58.3	No failure, suspended
A	15	2	5340N	53.1	No failure, suspended
	16	1	------	----	S/N given to set of races only
A	17	1	5340N	2.2	Diagonal Break)
A	18	1	------	0.3	Diagonal Break)Retainer
A	19	1	------	0.2	Hairline Crack)Misaligned
A	20	1	5340N	53.1	No failure, suspended
A	21	2	5340N	54.1	No failure, suspended
B	22	1	6008N	53.6	No failure, suspended
B	23	2	6008N	53.0	No failure, suspended
B	24	1	6008N	53.7	No failure, suspended
B	25	2	6008N	54.6	No failure, suspended
B	26	1	6008N	54.2	No failure, suspended
C*	27	2	6008N	53.8	No failure, suspended
C*	28	1	6008N	53.1	No failure, suspended
C*	29	2	6008N	53.0	No failure, suspended
C	30	1	6008N	32.6	Rig problem, suspended
C	31	2	6008N	0.2	Diag. break; infant failure
C	32	2	6008N	0.3	Diag. break; infant failure
C*	33	2	6008N	0.1	Diag. break; infant failure
C*	34	2	6008N	0.1	Diag. break; infant failure
B	35	2	6008N	55.3	No failure, suspended
C*	36	1	6008N	61.5	No failure, suspended
A**	37	1	6008N	20.7	Diagonal break
A**	38	2	6008N	53.3	No failure, suspended
A**	39	1	6008N	8.7	Diagonal break
A**	40	1	6008N	54.3	Radial break
A**	41	2	6008N	53.8	No failure, suspended
A**	42	1	6008N	14.1	Diagonal break
B	43	2	6008N	106.5	No failure, suspended
B	44	2	6008N	106.0	No failure, suspended
B	45	1	6008N	108.1	No failure, suspended

* Task IC design balls which were identifiable as having minimal stock removal by grinding

** Task IA design balls which were especially processed to provide 1.14 mm (.045") minimum stock removal by grinding

TABLE II (Continued)

DESIGN	BALL NO.	MACHINE	LOAD	HOURS	STATUS
B	46	2	6008N	106.1	No failure, suspended
B	47	1	6008N	106.7	No failure, suspended
A**	48	2	5340N	106.3	No failure, suspended
A**	49	1	5340N	108.3	No failure, suspended
A**	50	2	5340N	11.2	Diagonal Break
A**	51	2	5340N	33.6	Diag. break, probably related to a lubrication failure
C	52	1	6008N	106.3	No failure, suspended
C	53	2	6008N	106.0	No failure, suspended
D	54	1	6008N	1.0	Broken ball
D	55	2	6008N	0.5	Broken ball
D	56	1	5340N	8.8	Broken ball
D	57	2	5340N	1.1	Broken ball
D	58	2	4005N	0.15	Broken ball
D	59	1	4005N	0.2	Broken ball
D	60	1	4005N	14.6	Broken ball
D	61	2	4005N	0.2	Broken ball
D	62	2	4005N	53.1	No failure, suspended
D	63	1	4005N	53.1	No failure, suspended
D	64	2	4005N	24.7	Broken ball
D	65	1	4005N	2.1	Broken ball
D	66	1	4005N	5.9	Broken ball
C	67	1	6008N	108.4	No failure, suspended
C	68	2	6008N	104.0	No failure, suspended
B	69	1-V	6008N	0.17	Chunk broke out of loaded area
B	70	1-V	6008N	0.08	Chunk broke out of loaded area
B	71	1-V	5340N	0.10	Chunk broke out of loaded area
B	72	1-V	5340N	0.11	Spalled ball, cracks under spall
B	73	2-V	------	------	Skidded at start, rig prob.
B	74	1-V	4450N	0.65	Spalled ball, cracks under spall
B	75	1-V	4450N	0.30	Spalled ball
B	76	2-V	------	------	Skidded at start, rig prob.
B	77	1-V	3560N	15.9	Spalled ball, cracks under spall
B	78	1-V	3560N	11.6	Spalled ball, additional breakage under spall

"-V" signifies test rig set up with one V-groove race and one standard inner race.
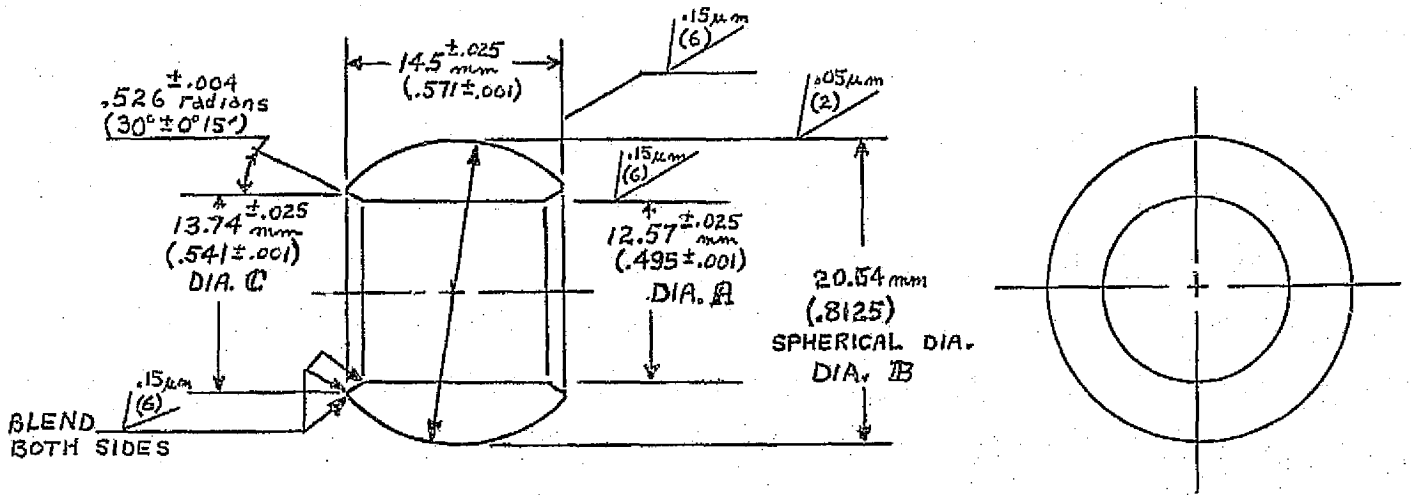
MATERIAL — M-50 TOOL STEEL CVM

DIA. A TO BE CONCENTRIC WITH DIA. B WITHIN .025 mm (.001) T.I.R.

DIA. C TO BE CONCENTRIC WITH DIA. A WITHIN .05 mm (.002) T.I.R.

FIGURE I - DESIGN A DRILLED BALL
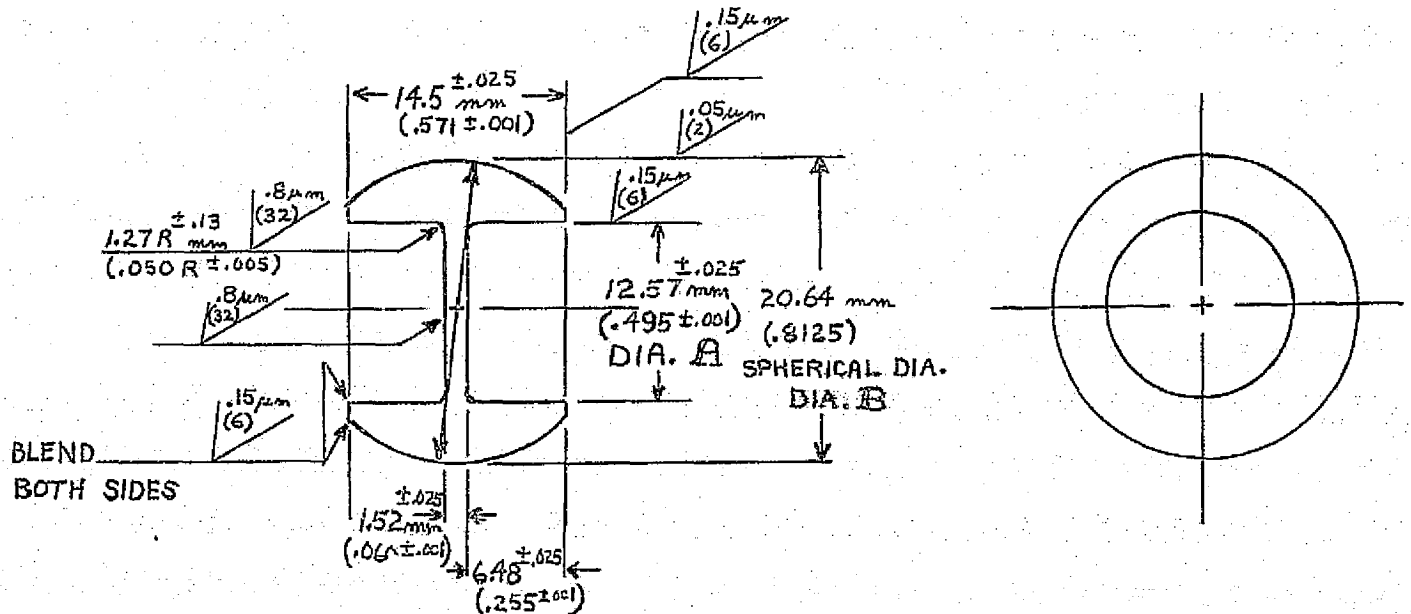
MATERIAL — M-50 TOOL STEEL CVM

DIA. A TO BE CONCENTRIC WITH DIA. B WITHIN .025 mm (.001) T.I.R.

FIGURE 2 - DESIGN B DRILLED BALL
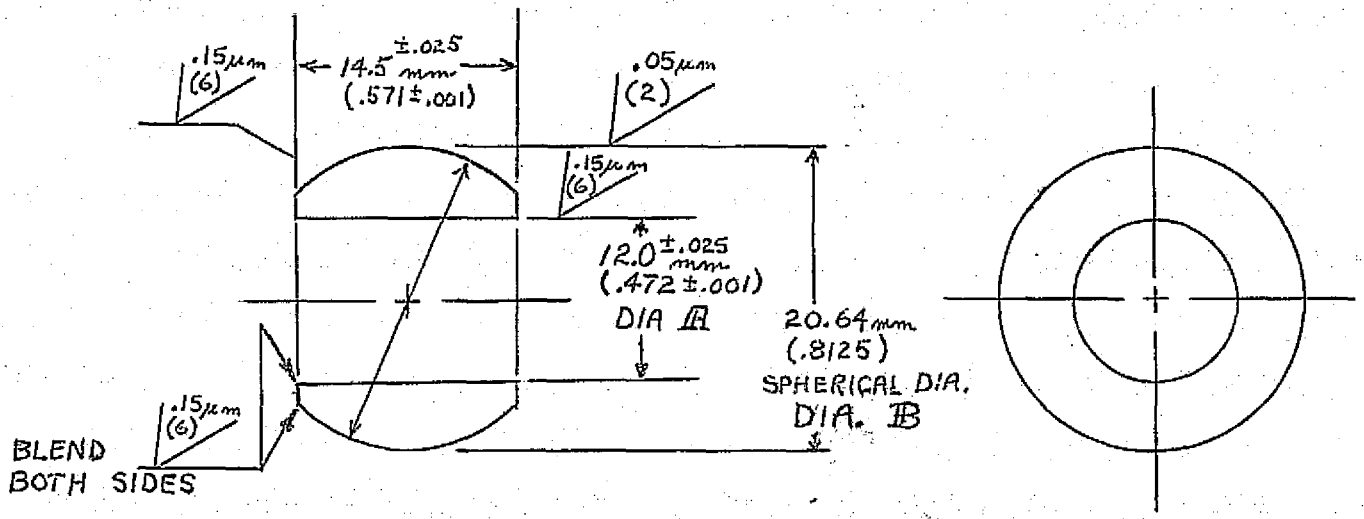
MATERIAL — M-50 TOOL STEEL   CVM
DIA. A TO BE CONCENTRIC WITH DIA. B WITHIN .025 mm (.001) T.I.R.

FIGURE 3 - DESIGN C DRILLED BALL

LOAD

ROLLING CONTACT
POSITIONER

Idler Shaft

Test
Ball

Drive
Shaft
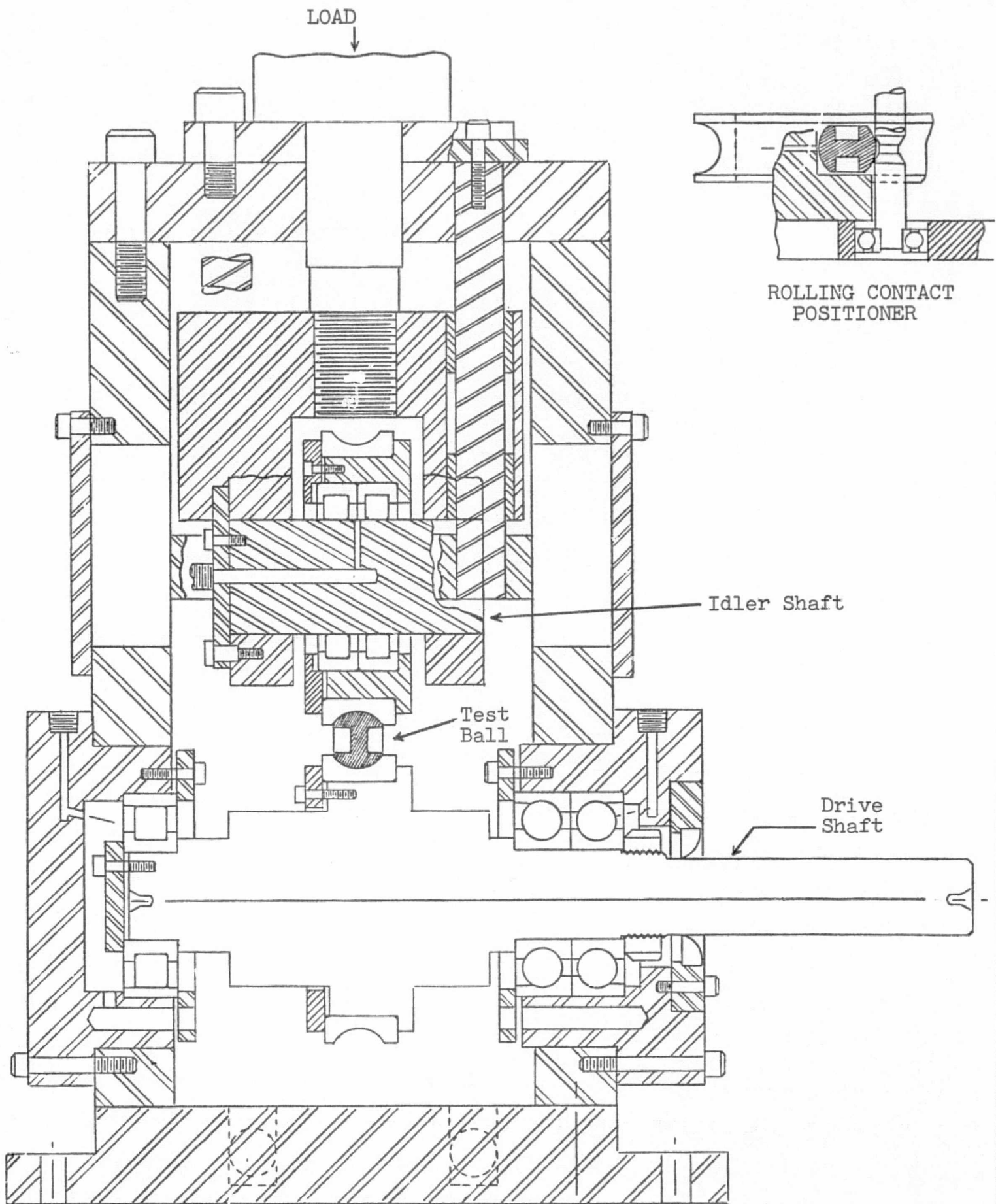
FIGURE 4 - SCHEMATIC OF MODIFIED ONE BALL TEST RIG

Loading
Cylinder

Idler
Shaft

Drive
Shaft
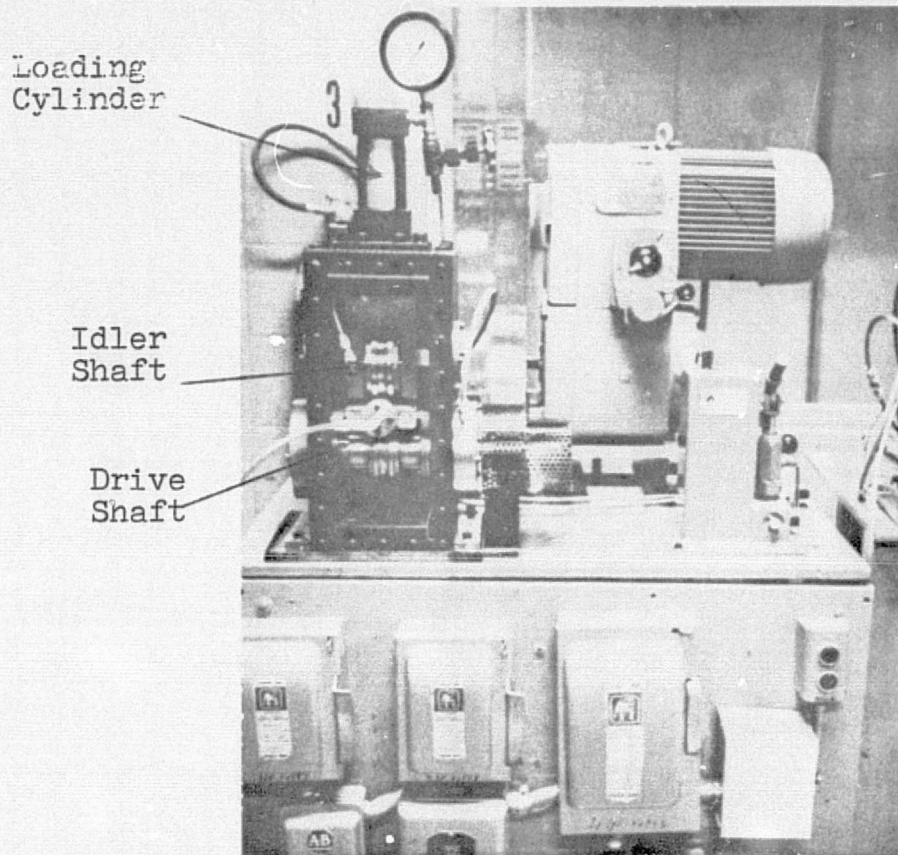
FIGURE 5 - Modified One Ball Test Apparatus

OUTER RACE
TEMPERATURE

TEST BEARING

UNDER RACE
DISCHARGE
OIL OUT

OIL
IN ←

COUPLING DRIVE

THRUST

LOAD

MRC 216-R
SUPPORT BEARING

MRC 116-KR
SUPPORT BEARING

LUBRICATING
OIL OUT
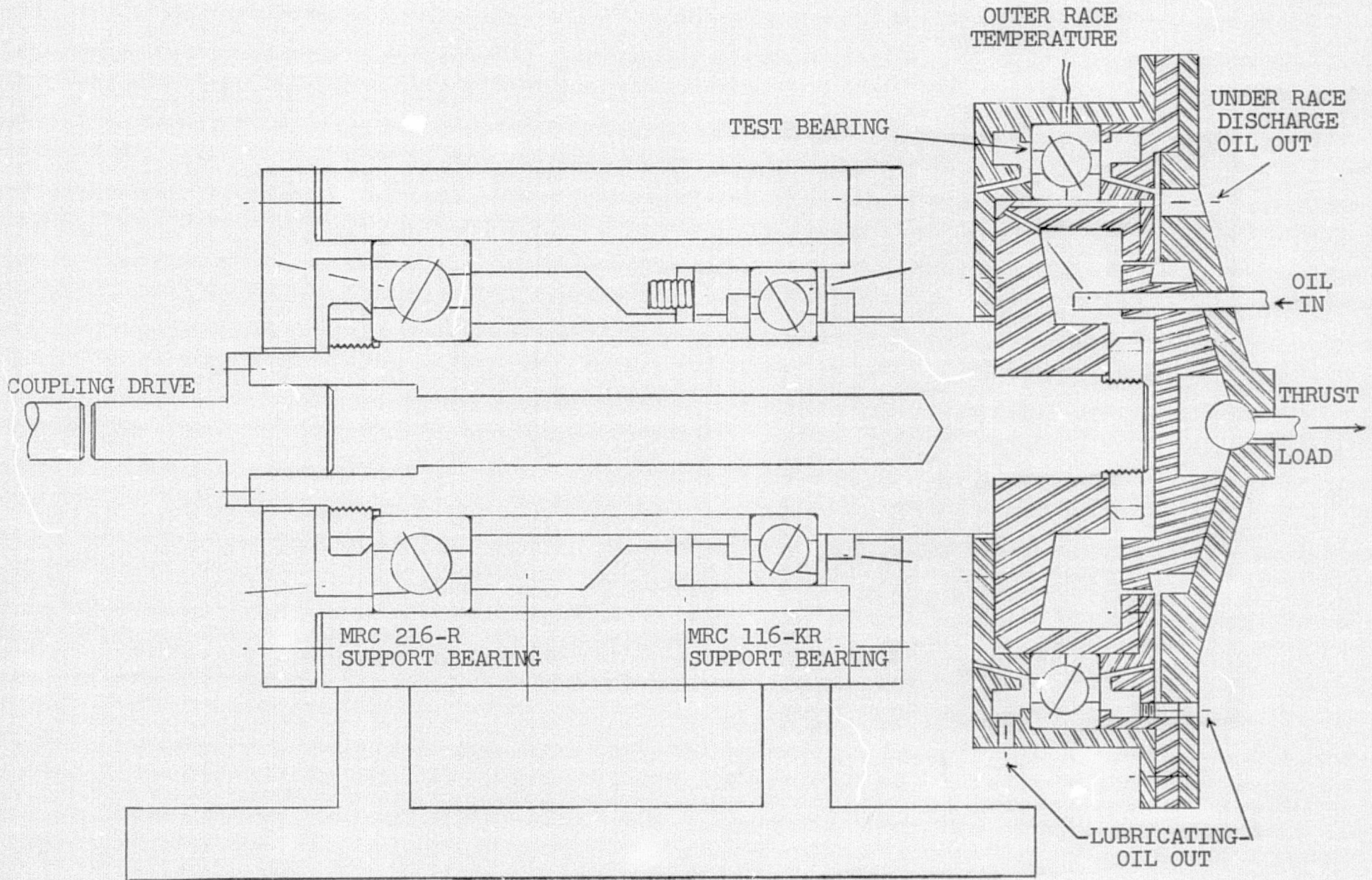
FIGURE 6 - TEST SPINDLE SCHEMATIC

Torque
Arm

Load
Cable
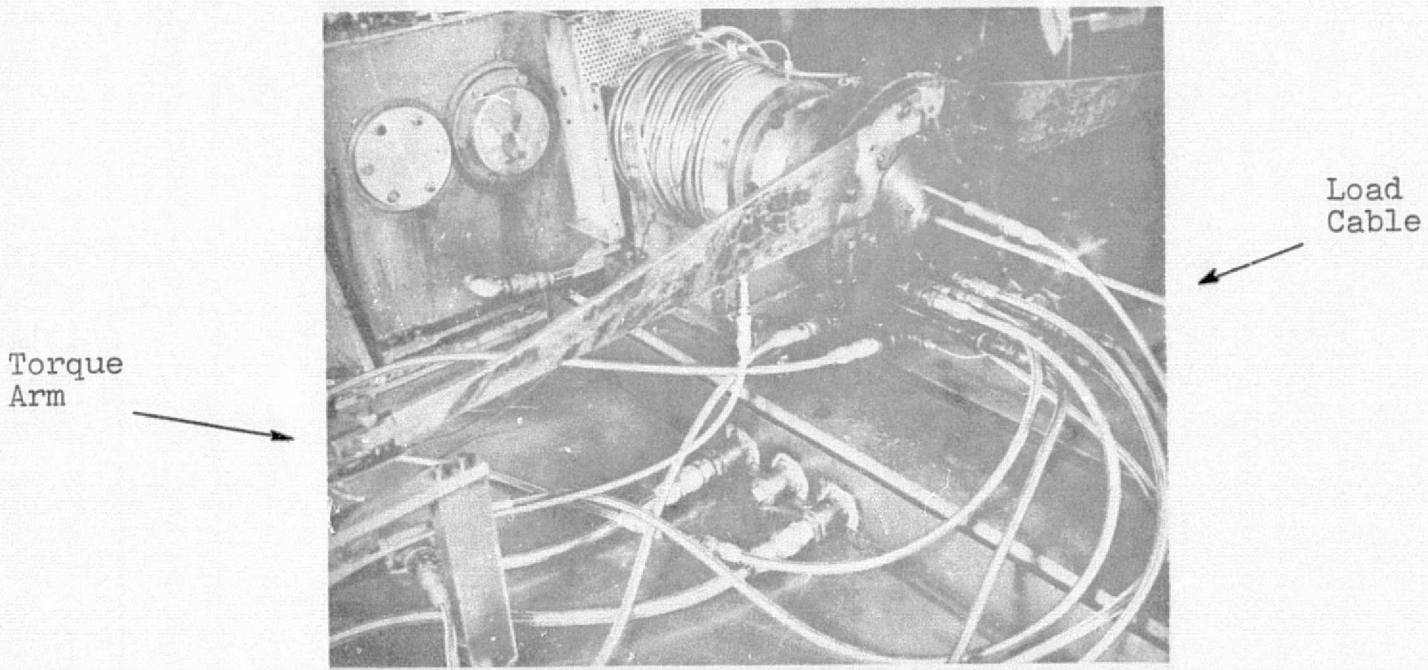
FIGURE 7 - Bearing Test Rig

ORIGINAL PAGE IS
OF POOR QUALITY

FIGURE 8

Tests of Drilled Balls Run on Modified One-Ball Test Rig

Design D Balls run at 4005N (900 pounds) 7 Failures out of 9 tests

Second Lot of Design A balls run at 6008 N (1350 pounds) radial load. 4 Failures out of 6 tests

Design A balls run at 6008 N (1350 pounds) radial load. (Original lot excluding infant failures). 3 Failures out of 5 tests

BALLS TESTED - STATISTICAL PER CENT

BALL LIFE - MILLIONS OF STRESS CYCLES

FIGURE 9 - Design B Ball No. 72, Run on a V-Groove Race,
with Spall Which Cracked Through to Bore.
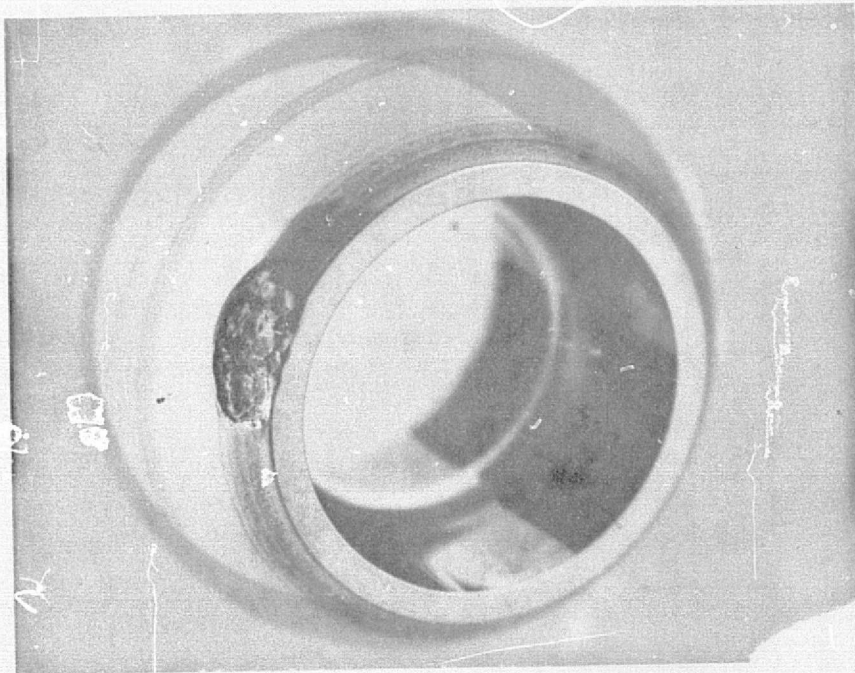
FIGURE 10 - Design B Ball No. 75, Run on a V-Groove Race,
with Fatigue Spall.
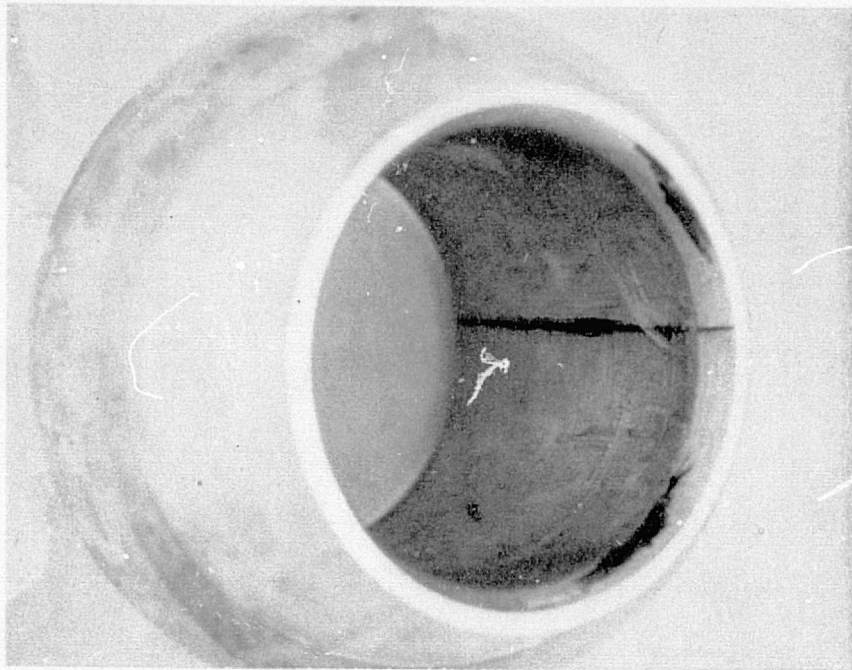
FIGURE 11 - Design A Ball No. 19, Showing Failure Which Did Not Progress to Ball Outer Surface. (Crack is accentuated with Magnaflux Solution)
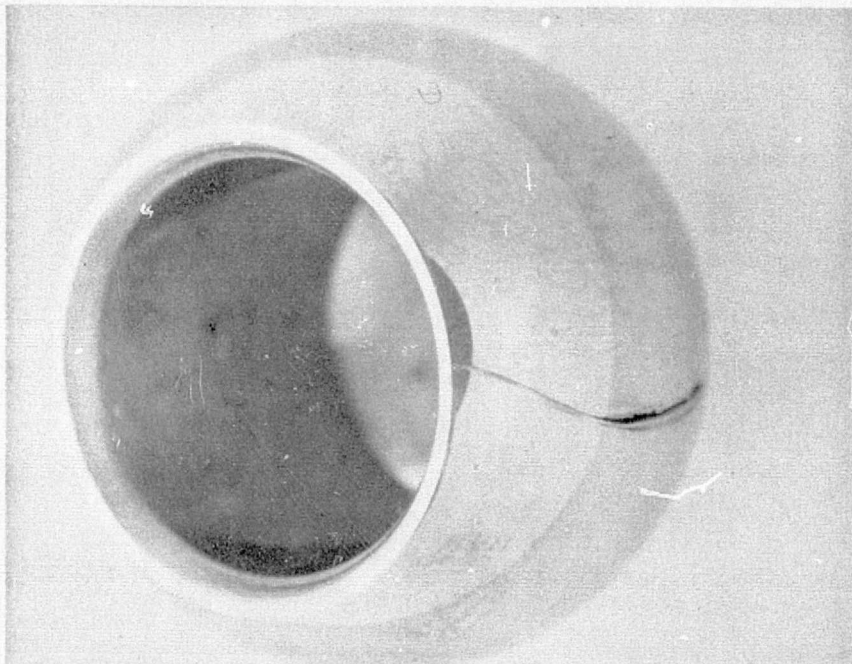
FIGURE 12 - Design A Ball No. 11, Showing Failure With Diagonal Crack.
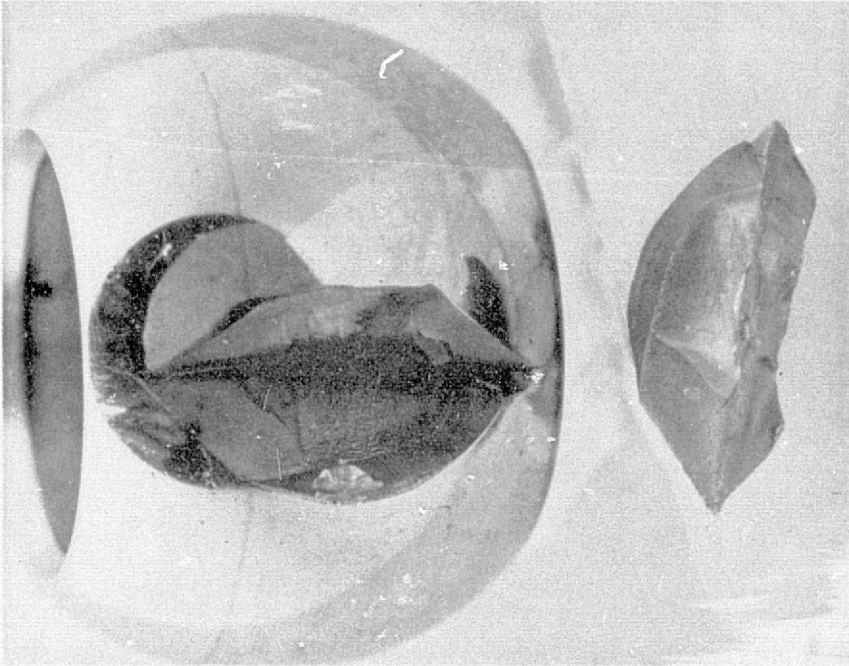
FIGURE 13 - Design A Ball No. 4, Showing Ball With Aggravated
Diagonal Break.
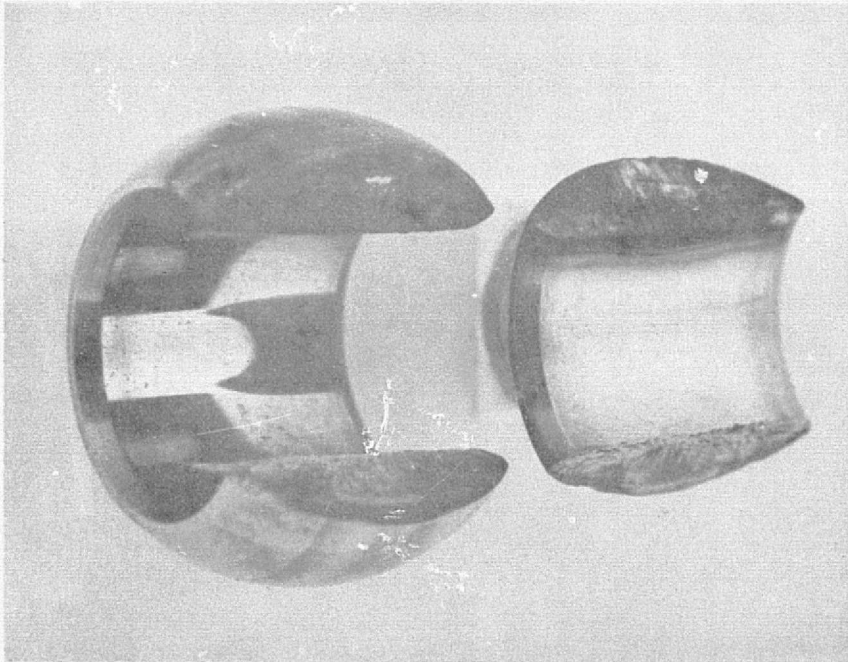
FIGURE 14 - Design A Ball No. 6, which Suffered Two Radial
Fractures. Initial Crack is Discolored from Frictional Heat.
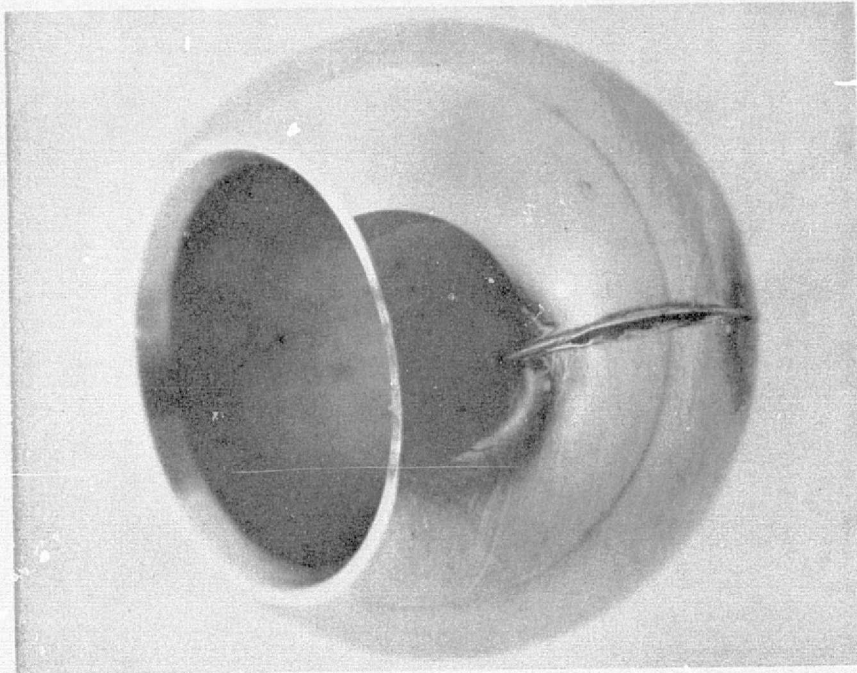
FIGURE 15 - Design A Ball No. 13, Showing Failure Which Overheated at the Crack.

FIGURE 16 - Design D Ball No. 58, Showing Non-Planar Crack in Bore of Carburized Ball. (Crack is accentuated with Magnaflux Solution)

41
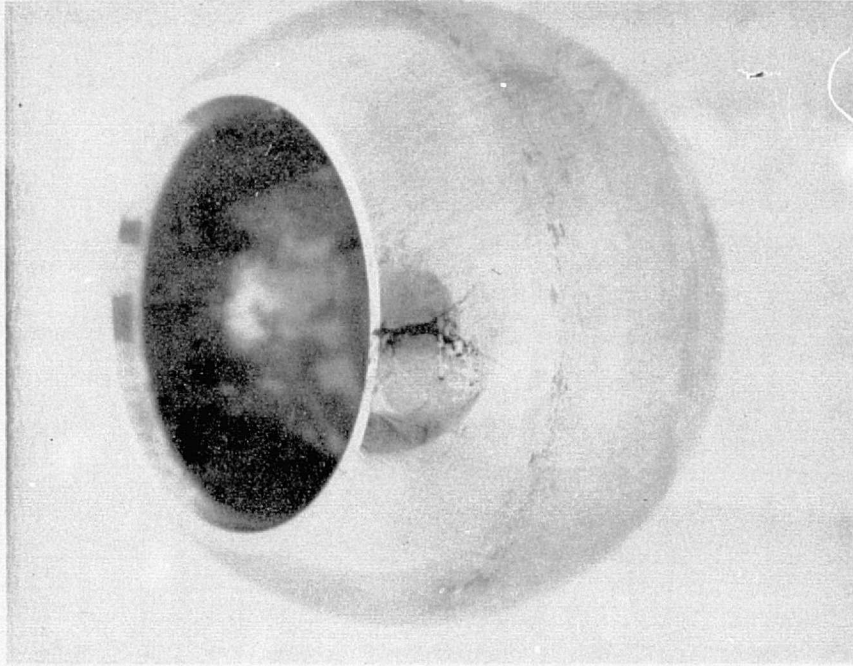
FIGURE 17 - Design D Ball No. 58, Showing Arrested Crack in Carburized Ball. (Crack is accentuated with Magnaflux Solution)
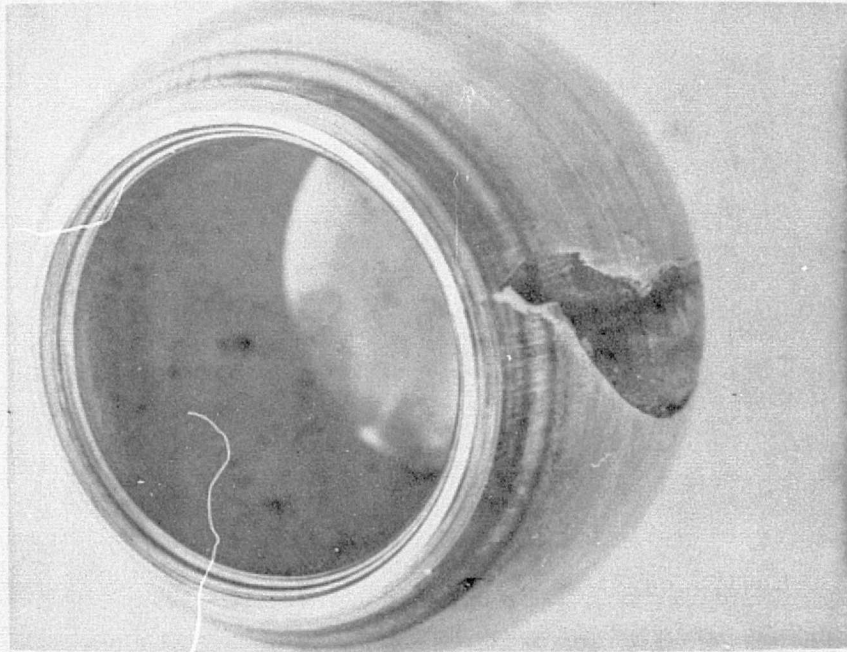
FIGURE 18 - Design D Ball No. 60, Showing Fractured Carburized Ball.
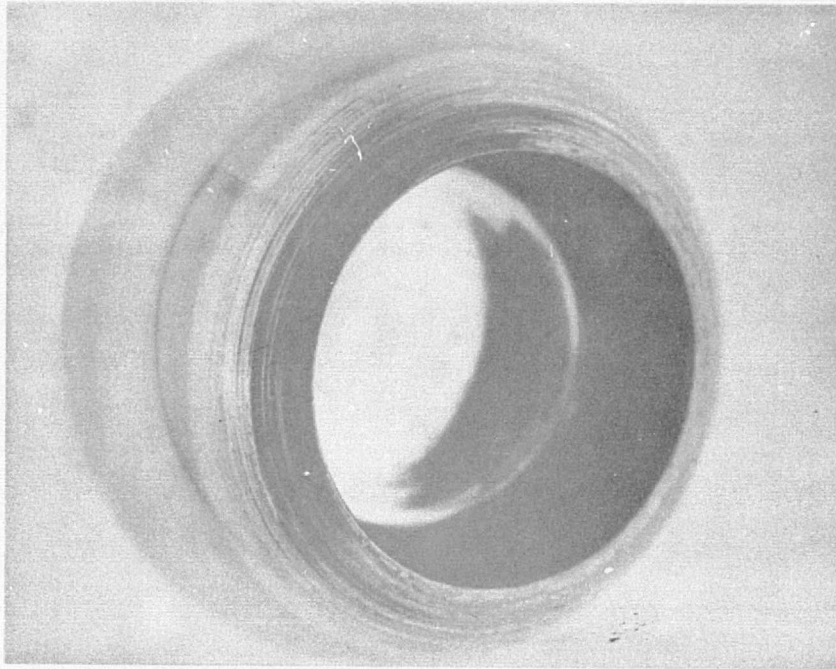
FIGURE 19 - Design B Ball from Ball Bearing Test, Showing Abraded Side which Scrubbed Cage Rib.

FIGURE 20 - Typical Damaged Ball Pocket Rib, from Contact with Tilted Design B Ball.
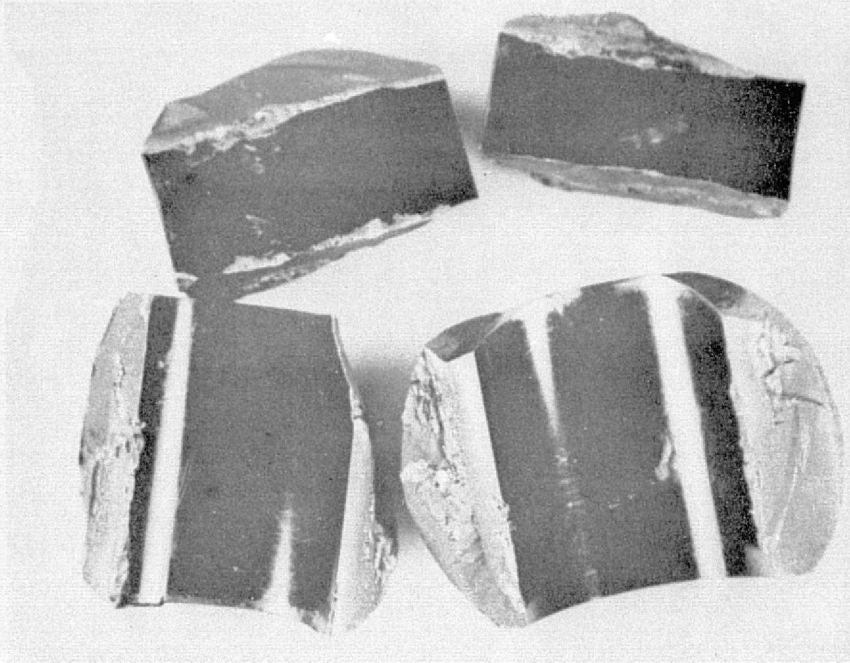
FIGURE 21 - Fractured Design C Ball After 28.9 Hours Operation in MRC 9130-UK-29 Ball Bearing at 20000 rpm with Full Bearing Thrust Load of 20500 N (6850 lb.)
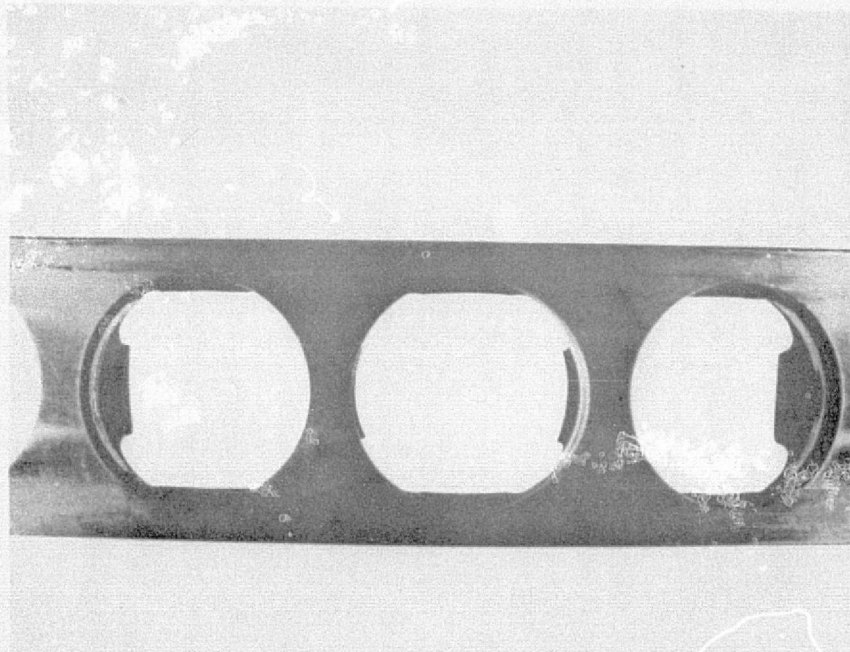

FIGURE 22 - Cage from MRC 9130-UK-29 Ball Bearing after 20 Hours Operation at Full Load and Speed. Cage was in Good Condition.
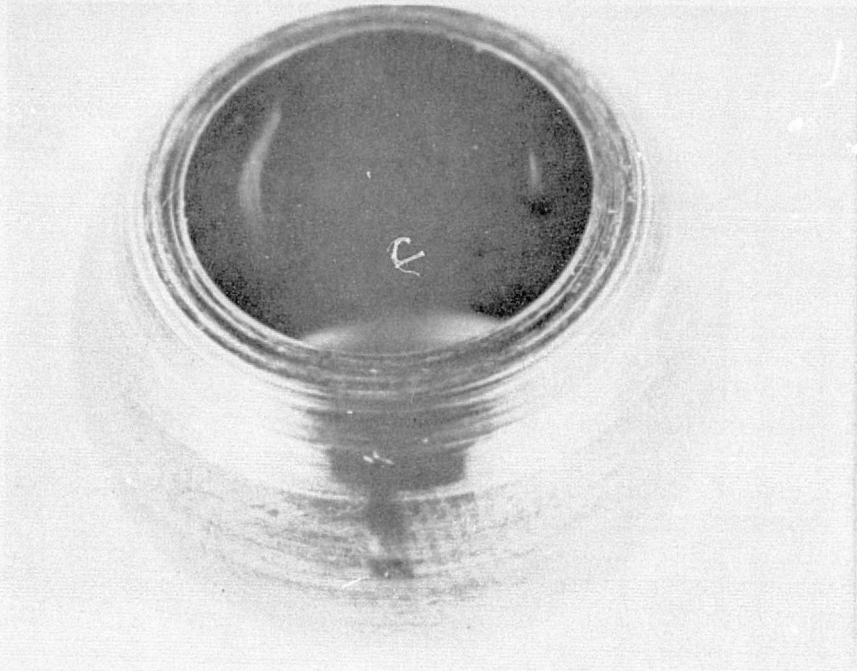
FIGURE 23 - Unbroken Design C Ball Removed from Bearing at Completion
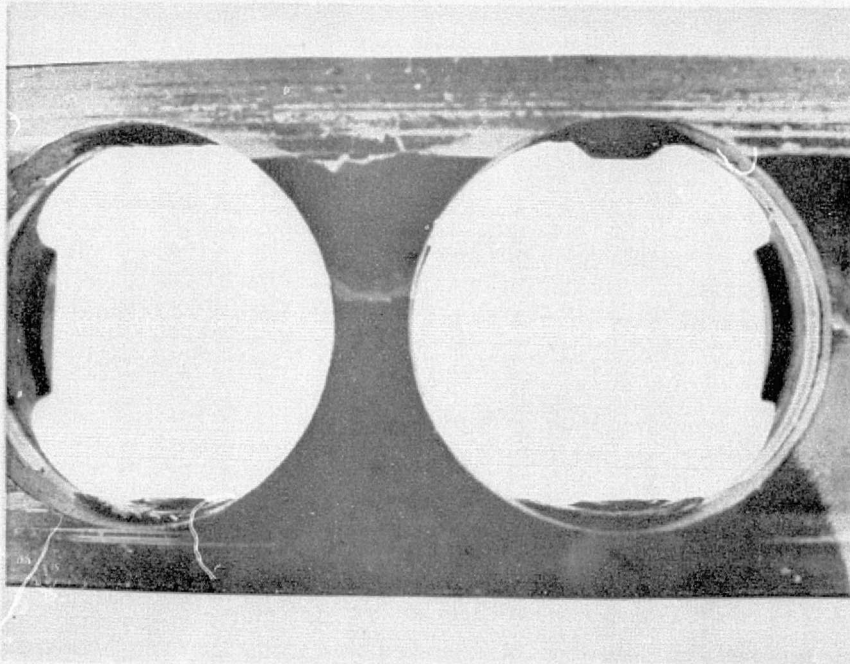of Test. Ball Shows Severe Contact with Cage Pocket Restraints.

FIGURE 24 - View of Cage After Completion of Test Showing Damaged
Pocket Restraints and O.D. wear.